Highly radioactive topaz rhyolites of the Toano Range, northeastern Nevada

JONATHAN G. PRICE, STEPHEN B. CASTOR

Nevada Bureau of Mines and Geology, University of Nevada, Reno, Nevada 89557-0088, U.S.A.

DAVID M. MILLER

U.S. Geological Survey, 345 Middlefield Road, Menlo Park, California 94025, U.S.A.

ABSTRACT

Highly radioactive topaz rhyolites of Miocene age are described from a new locality in the Toano Range of northeastern Nevada. Quartz phenocrysts are blackened by radiation damage. High magmatic Th and U concentrations (87 and 46 ppm, respectively) allow the rhyolites to be readily distinguished on aeroradiometric maps.

In addition to quartz, the rhyolites contain phenocrysts of sanidine, plagioclase, biotite, titanomagnetite, and rare fayalite. Vitrophyres have several unusual features: microphenocrysts of octahedral fluorite, rod- and worm-shaped microlite of iron oxide, and microlite of fayalite. Vapor-phase cavities in devitrified rocks contain topaz and quartz.

The rhyolites occur as lava flows and pyroclastic deposits that originated from at least two vents. Emplacement of a nonwelded lithic tuff with topaz-rhyolite composition preceded the lava flows. Two groups of lavas are defined by petrographic differences and trace-element compositions. Rocks from the group with relatively large quartz phenocrysts and smaller, less abundant biotite phenocrysts tend to be more enriched in some incompatible trace elements, notably Th and REE, than the other group.

Rocks that have undergone various amounts of postemplacement crystallization are locally enriched in elements that apparently were transported in the vapor phase, notably As, Sb, Au, and Hg. Because magma degassing, hydration of vitrophyres, vapor-phase crystallization, and devitrification can affect the rock composition, true magmatic abundances of these elements are uncertain.

INTRODUCTION

This study was undertaken to characterize, petrographically and chemically, rhyolites of the Toano Range in northeastern Nevada. The two groups of rhyolites that we can map and recognize in the field on the basis of differences in biotite content and size of quartz phenocrysts are chemically distinct. We report some unusual petrographic features in these rhyolites and compare their chemical compositions with those of other topaz rhyolites. Topaz rhyolites are typically more enriched in certain incompatible trace elements than are other high-silica rhyolites. The more incompatible-element enriched varieties of topaz rhyolites are the sources of elements in some ore deposits, notably Be and Sn (Christiansen et al., 1986). Upon examination of the aeroradiometric maps of Duval (1988), we suspected that the rhyolites of the Toano Range might be particularly radioactive topaz rhyolites. They are, indeed, some of the most Th- and U-rich topaz-bearing rhyolites that have been described. Proffitt et al. (1982) recognized the anomalously high U content of these rocks but did not identify them as topaz rhyolites.

FIELD RELATIONS

Rhyolites occur in the Toano Range as lava flows, pyroclastic rocks, and plugs. The flows overlie a package of Tertiary sedimentary and volcanic rocks (sandstones, tuffaceous sandstones, siltstones, limestones, and reworked tuff mapped as Ts_1 by Coats, 1987) and the Toano Springs pluton (Miller et al., 1990), a Cretaceous muscovite granite (Fig. 1).

We have studied the two plugs that were mapped by Glick (1987) and from which lava flows were erupted (Fig. 1). Other vents may be buried beneath the flows. The plugs occur in Proterozoic and Paleozoic metamorphic and sedimentary rocks, mostly quartzite and phyllite but with some limestone and dolomite. Columnar joints on the south side of the small plug have intersections that locally plunge horizontally, indicating cooling along a vertical contact with Precambrian metamorphic rocks. The rhyolite on the north side of this plug contains numerous blocks of quartzite. Pyroclastic rocks, including pumice-rich welded tuffs, occur at the base of the craggy peak comprising the large plug. Contacts between the pyroclastic rocks and the plug are obscure. The large plug has an exposed vertical extent of 170 m. The lava flows attain a maximum thickness of 50 m (near locality 37, Fig. 1) and are presently exposed over an area of approximately 40 km². Original erupted volume was probably on the order of 2 km³.

Lithic tuff, whose pumice is chemically and mineralogically similar to the lavas, occurs in the north-central part
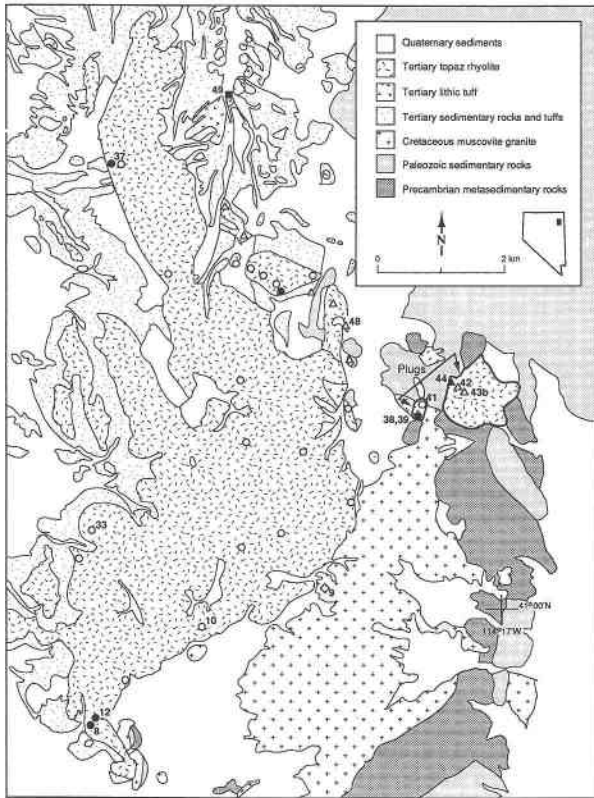
Fig. 1.   Geologic sketch map of the outcrop extent of topaz rhyolites of the Toano Range, Nevada (modified from Glick, 1987). Two identified plugs are outlined in bold lines on the eastern part of the map. Folds and faults in Paleozoic and Precambrian rocks and minor normal faults in Tertiary rocks are not shown for simplicity. Symbols indicate the types of samples that have been petrographically examined; numbers, without the J89 or J90 prefix, identify samples for which chemical analyses are reported in Table 1. Solid circles = vitrophyres from the small plug and petrographically similar flows (samples J89-8, J90-12, and J90-39); open circles = devitrified rhyolite from the small plug and petrographically similar flows (samples J90-10, J90-33, J90-37, J90-38, and J90-41); open triangles = devitrified rhyolite from the large plug and petrographically similar flow (J90-42, J90-43b, and J90-48); closed triangle = pyroclastic unit from base of large plug (J90-44); closed square = pumice from nonwelded tuff in northern outcrop area (J90-49).

of the study area (Fig. 1). This nonwelded tuff overlies tilted tuffaceous sedimentary rocks along a nearly horizontal contact. Lithic clasts include Precambrian and Paleozoic metamorphic rocks and the Cretaceous muscovite granite. Because the tuff lacks welding and flattening of pumice blocks, we interpret it to be an airfall tuff. The tuff is composed of upper and lower lithic-rich units and a middle pumice-rich unit; cumulative thickness is less than or equal to 30 m. Thickness and clast size in the tuff decrease northward and indicate an eruptive site south of the outcrop, perhaps at the mapped plugs. A different lithic tuff, one containing only clasts of rhyolite petrographically similar to the small plug, crops out in a small

area surrounded by Tertiary sedimentary rocks and airfall tuffs (between localities 48 and 49, too small to be mapped on Fig. 1).

PETROGRAPHIC CHARACTERISTICS

The rhyolites contain phenocrysts, in decreasing abundance, of blackened (deeply smoky) quartz, sanidine, plagioclase, biotite, titanomagnetite (generally oxidized to hematite + ilmenite), and rare fayalite (positively identified as a phenocryst phase in only one of 44 thin sections). Total phenocryst content is approximately 15%, and quartz accounts for approximately 60% of the phenocryst volume. Quartz phenocrysts are anhedral and commonly resorbed, whereas sanidine, plagioclase, and biotite phenocrysts are subhedral to the euhedral.

Fresh devitrified rocks have a light gray to medium light gray groundmass composed primarily of quartz and alkali feldspar. Vitrophyres locally contain microphenocrysts of octahedral fluorite (Fig. 2a) and fayalite (Fig. 2b) plus rod- and worm-shaped, flow-aligned microlite of iron oxide. Some microlite samples have been positively identified as hematite, both optically (from their red internal reflection) and by quantitative energy dispersive analysis with a scanning electron microscope. Iron oxide microlite lacking red internal reflection is probably magnetite, and all of the hematite microlite samples may be oxidized magnetite grains. We identified small crystals of pyrite in one sample of black, hydrated vitrophyre.

Although magmatic fluorite has been recognized in some other topaz rhyolites, fayalite is rare in these rocks (Christiansen et al., 1986). In rhyolites of the Toano Range, fayalite is most readily visible in vitrophyres. Its composition as nearly pure fayalite, $(Fe_{1.83}Mn_{0.08}Ca_{0.08}Mg_{0.007})SiO_4$, was determined by quantitative energy dispersive analysis with a scanning electron microscope. It occurs as discrete, pale green microlite in some samples and as small crystals attached to iron oxide microlites (Fig. 2b) in others. This texture suggests that the fayalite crystals nucleated on the iron oxide microlites.

Biotite occurs in several forms: as brown- and, generally smaller, green-pleochroic phenocrysts; as brown grains in glomerocrysts with plagioclase, alkali feldspar, quartz, and traces of zircon; as brown inclusions in quartz and feldspars; and as generally green-pleochroic grains intergrown with quartz and feldspar in the groundmass of devitrified rocks. In some devitrified rocks, clots of green groundmass biotite surrounding magnetite phenocrysts suggest that these biotite grains nucleated at a site of high Fe content. Some samples contain feldspar-quartz devitrification spherules that appear to have nucleated on small biotite phenocrysts.

Topaz occurs as euhedral crystals as long as 5 mm in vapor-phase cavities, generally with quartz. We recognize topaz in samples from the southwestern and northern outcrop areas but not from the eastern outcrop area. Most vapor-phase cavities are lined with euhedral quartz, without topaz.

At least two types of rhyolite are petrographically dis-

tinguishable, both in plugs and flows. The smaller of the two plugs and most of the lava flows contain relatively large (up to 6 mm in diameter) quartz phenocrysts and biotite microphenocrysts that are generally too small to be recognized in hand specimen. The larger plug and petrographically similar flow contain smaller (generally 0.5–2.5-mm and rarely up to 3.5-mm) quartz phenocrysts and biotite phenocrysts up to 2 mm long. The grain-size distinction between the two types of rhyolite is evident in the percentage of quartz phenocrysts greater than 1 mm in diameter: 35–65% for the rhyolite with large quartz crystals vs. 14–36% for the rhyolite with small crystals. The small-quartz, large-biotite flows have been mapped only in scattered outcrops northwest of the large plug (triangles in Fig. 1). Most outcrops are rhyolite that contains large quartz phenocrysts and lacks macroscopic biotite (circles in Fig. 1).

The pyroclastic rocks that crop out adjacent to the large plug contain quartz and biotite phenocrysts of the same size as phenocrysts in that plug. In thin section, some of the resorbed quartz phenocrysts in the pyroclastic rocks appear to be broken.

The nonwelded, lithic tuff in the north-central part of the study area contains a phenocryst assemblage similar to the topaz rhyolite flows: resorbed quartz, sanidine, plagioclase, and brown-pleochroic biotite. The quartz in this rock is somewhat smoky but not blackened as in the topaz rhyolites. Large biotite suggest that the tuff was erupted from the vent marked by the large plug.

CHEMICAL ANALYSES

Analyses of 14 rocks from this area are reported in Table 1. Care was taken in the field to remove any obvious weathering rind from rocks sampled for chemical analyses. Sample preparation and analyses were performed by commercial laboratories (Bondar-Clegg for most analyses, XRAL Activation Services for Au) using quality assurance procedures established for the Geochemical Sampling and Characterization Program at the Nevada Bureau of Mines and Geology. Analyses of standard reference materials and control samples are reported by Bonham et al. (1990).

The following analytical techniques were used: multiple acid total digestion plus direct current plasma spectroscopy for major oxides; gravimetric analysis for loss on ignition; Leco technique for total S; cold vapor atomic absorption spectrophotometry for Hg; multiple acid digestion and MIBK extraction followed by atomic absorption spectrophotometry for Tl; multiple acid total digestion plus atomic absorption spectrophotometry for Be; multiple acid total digestion plus inductively coupled plasma-atomic emission spectroscopy for Li, V, Cr, Co, Ni, Cu, Zn, Ga, Sr, Y, Nb, Cd, Sn, Ba, Pb, and Bi; instrumental neutron activation analysis for Sc, As, Se, Br, Rb, Zr, Mo, Ag, Sb, Te, Cs, La, Ce, Sm, Eu, Tb, Yb, Lu, Hf, Ta, W, Ir, Th, and U; and neutron activation followed by radiochemical separation by fire assay for Au. Our quality-assurance data on replicate control samples in-
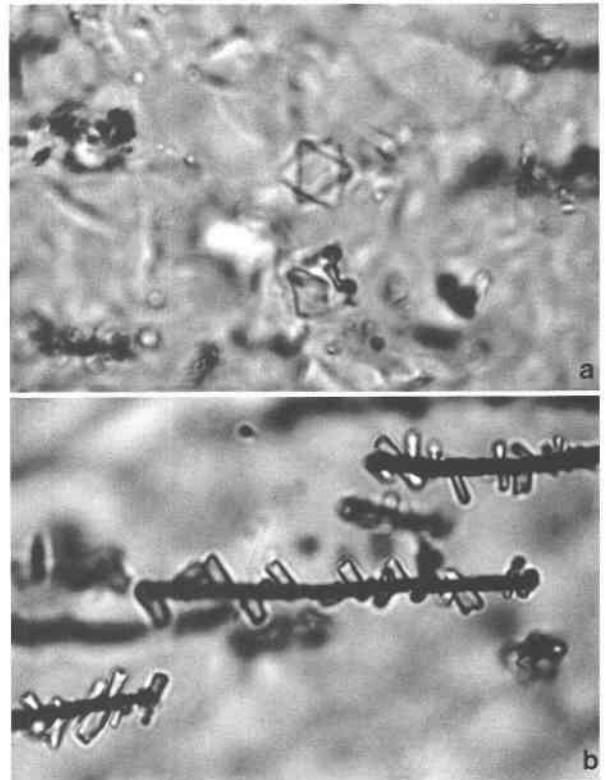

Fig. 2. Photomicrograph of (**a**) a fluorite microphenocryst and (**b**) fayalite microlite samples attached to iron oxide microlite samples in glass, sample J89-8. View in **a** is perpendicular to a (111) triangular face on a fluorite octahedron, with the underlying (111) face forming a six-pointed star in two dimensions. The edge of the octahedron is 8 μm long. These octahedral crystals do not occur in all samples of vitrophyre; they have been recognized from the southern, central, and northern outcrop areas (solid circles in Fig. 1). In **b** the central iron oxide rod is 44 μm long. In this sample, fayalite appears to have nucleated on magnetite. In some glass samples, fayalite occurs as independent microphenocrysts not attached to iron-oxide microlite. Both fluorite and fayalite were confirmed by energy dispersive analysis with a scanning electron microscope.

dicate that the reproducibility of the Au analyses is ±0.5 ppb.

At least two of the analyzed samples are not representative of magmatic compositions. Sample J90-41 is a breccia that contains fragments of Paleozoic quartzite and perhaps other sedimentary rocks in a matrix of rhyolite; it is not included in the plots illustrating chemical comparisons. Sample J90-49, pumice from the nonwelded tuff, contains abundant secondary calcite. Sample J90-48, a devitrified flow, is distinctly higher in silica and lower in K_2O than other samples and may have undergone considerable vapor-phase alteration. With these exceptions and the exception of sample J90-9, the Cretaceous muscovite granite, other samples in Table 1 are representative of the topaz rhyolites of the Toano Range.

TABLE 1. Chemical compositions of igneous rocks from the Toano Range, Elko County, Nevada

Sample no.	J89-8	J90-12	J90-39	J90-10	J90-33	J90-37	J90-38	J90-41	J90-42	J90-43b	J90-48	J90-44	J90-49	J90-9
						Oxides (%, normalized, volatile free)									
SiO$_2$	76.4	76.5	76.7	77.9	76.3	77.3	76.4	80.4	77.6	77.6	79.5	76.7	71.7	75.4
TiO$_2$	0.11	0.10	0.07	0.10	0.09	0.07	0.07	0.12	0.08	0.08	0.06	0.05	0.04	0.09
Al$_2$O$_3$	12.8	12.5	12.5	12.0	12.3	12.2	12.1	8.8	11.6	11.9	10.2	12.1	12.2	14.5
Fe$_2$O$_{3tot}$	1.15	1.42	1.31	1.30	1.42	1.15	1.30	1.22	1.16	1.19	1.15	1.28	1.25	0.36
MnO	0.03	0.03	0.02	0.03	0.03	0.02	0.03	0.04	0.03	0.03	0.02	0.04	0.04	0.01
MgO	0.18	0.06	0.06	0.03	0.10	0.03	0.02	0.19	0.04	0.05	0.11	0.04	0.23	0.08
CaO	0.66	0.66	1.07	0.13	0.95	0.26	0.54	1.67	0.29	0.22	1.35	0.19	5.98	0.44
Na$_2$O	3.18	3.21	2.81	3.46	3.49	3.39	2.18	0.69	2.14	2.73	2.94	2.88	2.07	4.35
K$_2$O	5.29	5.41	5.43	4.79	5.27	5.40	7.36	6.59	6.98	6.19	4.36	6.50	6.33	4.48
P$_2$O$_5$	0.20	0.10	0.06	0.24	0.07	0.14	0.03	0.27	0.05	0.09	0.33	0.17	0.11	0.26
LOI	3.38	3.00	4.50	0.88	0.84	0.63	0.88	2.21	0.70	0.55	1.61	0.59	7.85	0.88
Total	97.4	98.3	99.7	97.9	100.0	98.8	99.4	99.4	99.1	99.2	98.9	98.1	98.8	98.5
						Trace elements (ppm)									
Li	36	25	110	70	120	120	110	44	78	93	73	140	37	<1
Be	27	21	26	17	19	24	18	20	12	20	13	26	24	4.3
F	5900	4700	4900	2200	2400	3100	1900	800	2000	1800	600	2200	1000	1400
S	400	300	200	<200	200	200	<200	200	600	200	200	200	200	<200
Sc	2.7	2.5	2.7	2.2	2.7	2.4	2.4	2.5	4.3	4.9	4.1	3.6	3.8	1.3
V	<1	<1	<1	<1	19	7	3	10	1	<1	29	<1	3	<1
Cr	3	<1	<1	<1	1	<1	<1	7	1	<1	<1	<1	2	2
Co	<1	<1	<1	2	3	<1	<1	2	<1	<1	3	1	<1	<1
Ni	1	<1	<1	<1	<1	<1	<1	6	<1	2	<1	<1	2	<1
Zn	47	47	61	40	56	40	56	49	55	56	58	64	73	6
As	2.4	1.3	1.2	3.6	18	3	14	9.2	60	7.7	4.4	1.8	1.6	1.0
Br	0.7	<0.5	<0.5	<0.5	<0.5	0.8	<0.5	<0.5	1.1	<0.5	<0.5	<0.5	1.9	<0.5
Rb	930	800	860	940	840	890	890	750	740	750	560	1040	870	230
Sr	15	<1	30	<1	11	6	15	26	12	12	14	11	39	116
Y	99	180	140	74	120	35	150	110	77	56	160	30	110	10
Nb	87	80	70	87	67	74	71	57	77	84	75	73	71	19
Sb	0.4	0.2	0.3	2.2	0.5	0.3	0.9	0.9	2.9	1.5	0.2	0.4	0.3	0.2
Cs	18	14	25	8	10	8	6	20	11	6	7	16	16	3
Ba	88	41	32	39	50	220	49	110	130	58	39	43	12	790
La	47	58	50	48	67	49	46	43	30	25	26	20	20	12
Ce	96	120	92	92	140	51	90	89	83	69	66	52	48	27
Sm	13	15	14	8.5	18	8.2	14	12	12	11	12	8.9	9.1	3.0
Tb	3.8	4.4	4.4	2.1	5.0	1.6	4.1	4.1	3.8	2.3	4.2	1.9	3.8	0.5
Yb	28	23	28	17	22	7	28	28	19	12	22	11	27	<2
Lu	2.7	2.4	3.5	2.3	3.2	0.6	3.3	3.2	1.8	1.0	2.5	0.9	2.6	<0.6
Hf	7	7	7	7	8	8	8	7	6	6	6	6	6	1
Ta	17	13	14	16	13	15	13	12	9.4	10	8.4	15	14	3
W	4	5	4	4	<1	4	2	4	5	<1	2	5	5	3
Au	0.0002	<0.0001	0.0004	0.0025	0.0005	0.0003	0.0003	0.0008	0.0013	0.0004	0.0002	0.0003	0.0006	0.0009
Hg	0.019	0.011	<0.010	0.195	0.055	<0.010	0.046	0.097	0.056	0.028	<0.010	0.025	<0.010	0.027
Tl	4.3	4.3	7.5	2.5	2.4	2.7	3.8	3.2	0.9	3.2	1.9	4.0	4.8	0.9
Pb	93	98	75	110	87	79	78	38	75	72	64	93	83	59
Th	84	90	85	73	100	96	83	78	65	64	60	50	48	9.0
U	48	44	46	18	21	28	47	48	32	26	23	23	38	4.7

Note: Small plug and petrographically similar flows: J89-8 = dark gray, perlitic, hydrated vitrophyre; base of flow; contains fluorite microphenocrysts. J90-12 = black, perlitic, hydrated vitrophyre; float, probably from base of flow. J90-39 = black, perlitic, hydrated vitrophyre; small plug. J90-10 = devitrified, flow-banded rhyolite; contains minor vapor-phase quartz. J90-33 = devitrified, flow-banded rhyolite; contains minor vapor-phase quartz. J90-37 = devitrified, flow-banded rhyolite; contains minor vapor-phase quartz. J90-38 = devitrified, flow-banded rhyolite with <1% quartzite rock fragments; small plug. J90-41 = rhyolite vent breccia; contains approximately 20% quartzite rock fragments; small plug. Large plug and petrographically similar pyroclastic rocks and flow: J90-42 = devitrified, flow-banded rhyolite; contains minor vapor-phase quartz; float, base of plug. J90-43b = devitrified, nonbanded rhyolite; top of exposed plug. J90-48 = devitrified, nonbanded rhyolite flow; contains minor secondary carbonate. J90-44 = pyroclastic rhyolite, devitrified; west of main plug. J90-49 = pumice from nonwelded, vitric lithic tuff; contains abundant secondary carbonate. J90-9 = Cretaceous muscovite granite, for comparison. Values for many trace elements were below detection limits (Cu < 20 ppm; Ga < 25 ppm; Se < 5 ppm; Zr < 200 ppm, except J90-33 with 450 ppm; Mo < 1 ppm; Ag < 2 ppm, except J90-49 with 2 ppm; Cd < 1 ppm; Sn < 20 ppm; Te < 10 ppm; Eu < 2 ppm; Ir < 0.05 ppm; Bi < 35 ppm).

CHEMICAL COMPARISONS

The rhyolites of the Toano Range are chemically similar to other topaz rhyolites. They are all high-silica rhyolites. Like other topaz rhyolites, those in the Toano Range are enriched in Li, Be, F, Zn, Rb, Y, Nb, Cs, and heavy REE, Ta, Th, and U (see Table 1) relative to most other rhyolites. They fall into the middle range of topaz rhyolites from Utah in terms of Nb and Rb (Fig. 3), but some

of the rhyolites of the Toano Range are exceptionally rich in U, Th, and K (Fig. 4, Table 1). Rocks with large quartz phenocrysts and sparse, small biotite phenocrysts (from the small plug and petrographically similar flows) tend to have higher Th concentrations than other rocks. The average Th content of seven large-quartz rhyolites is 87 ± 9 ppm. Assuming that some U may have been leached from the somewhat oxidized, devitrified rocks, the three
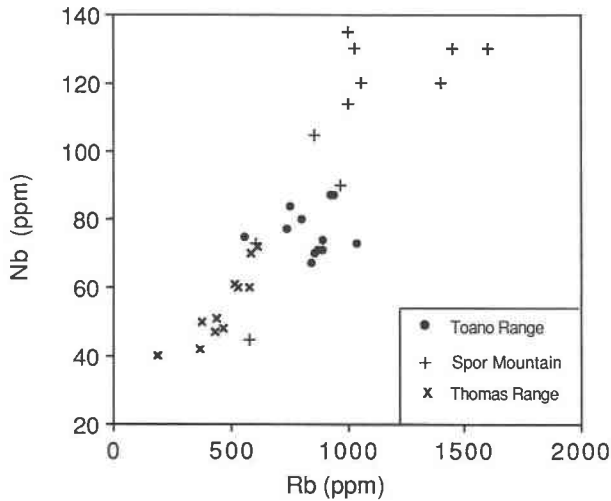
Fig. 3. Comparison of Nb and Rb in rhyolites of the Toano Range, Nevada (solid circles), with topaz rhyolites from the Thomas Range (crosses) and Spor Mountain, Utah (plus signs), from Christiansen et al. (1984).
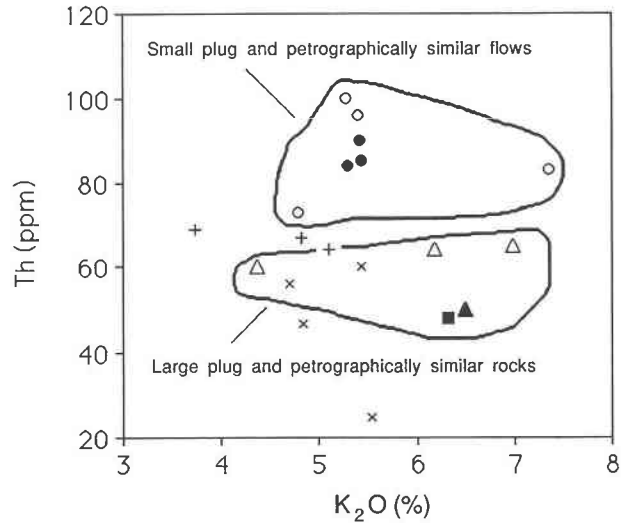

Fig. 4. Comparison of Th and K_2O in rhyolites of the Toano Range with topaz rhyolites from Utah. Symbols as in Figure 1. Topaz rhyolites from the Thomas Range (crosses) and Spor Mountain, Utah (plus signs), are from Christiansen et al. (1984). K_2O values are recalculated to a volatile-free basis.

vitrophyres probably yield a better average magmatic U content: 46 ± 2 ppm.

Rhyolites of the Toano Range have flat REE patterns with pronounced negative Eu anomalies. These patterns are characteristic of topaz rhyolites (Fig. 5). With the exception of sample J90-37, rocks with large quartz phenocrysts tend to have higher REE concentrations than those with small quartz phenocrysts. The rhyolites are only mildly peraluminous (Table 1), as are most topaz rhyolites (Christiansen et al., 1986). In contrast, the nearby Cretaceous muscovite granite is strongly peraluminous and has distinctly different trace element contents (Table 1; Lee et al., 1981).

The one analyzed pyroclastic rock, a pumice-rich welded tuff (J90-44 in Table 1), is chemically similar to the flow rocks of the nearby large plug (samples J90-42 and J90-43b). Pumice from the nonwelded lithic tuff (J90-49), located 6 km north of the large plug and occurring beneath the rhyolite flow, is also chemically similar. It is enriched in Li, Be, Rb, Cs, heavy REE, Ta, Tl, Th, and U, as are the topaz rhyolites.

The chemical analyses confirm the petrographic observation of at least two magma compositions: (1) a more evolved type with relatively large quartz phenocrysts (samples J89-8, J90-10, J90-12, J90-33, J90-37, J90-38, and J90-39) probably erupted from a vent occupied by the small plug, and (2) a less evolved type (samples J90-42, J90-43b, J90-44, and J90-48) erupted from a vent occupied by the large plug.

It is noteworthy that As and Sb are enriched only in the devitrified rocks and are uniformly low in hydrated vitrophyres and pyroclastic rocks (Fig. 6). The devitrified rocks are also locally enriched in certain other elements, notably Au and Hg (see Table 1). These four elements are characteristic pathfinder elements for epithermal gold

deposits. One explanation for this difference is that the vapor phase, which precipitated topaz and quartz in vugs, presumably during devitrification, transported and precipitated these elements. The devitrified rocks are enriched, relative to the average of the three analyzed vitrophyres, by as much as 37× in As, 14× in Hg, 11× in Au, and 10× in Sb. As an alternative explanation, it is possible that the differences between devitrified rocks and
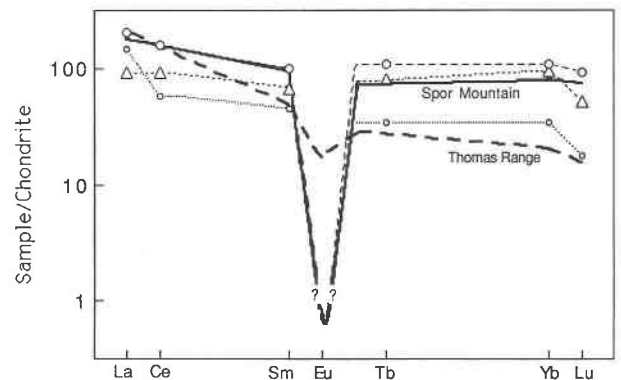

Fig. 5. Rare earth element concentrations in selected samples: large open circles = devitrified rhyolite from flow in western outcrop area and petrographically similar to the small plug (sample J90-33); small open circles = devitrified rhyolite from flow in northern outcrop area and petrographically similar to the small plug (sample J90-37); open triangles = devitrified rhyolite from the large plug (J90-42). For comparison, solid lines are samples SM-35 and SM-61a, topaz rhyolites from Spor Mountain and the Thomas Range, respectively (from Christiansen et al., 1984). The Eu anomaly for the Toano samples, which is shown as equal to that for Spor Mountain, is uncertain; none of the rhyolite samples exceeds the detection limit (2 ppm).
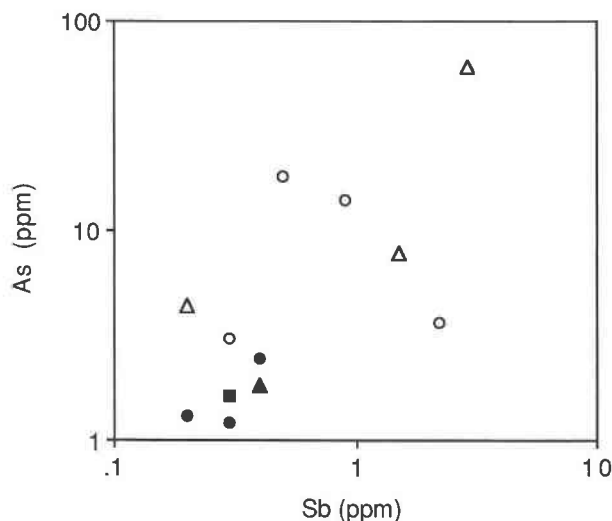
Fig. 6. As and Sb in rhyolites of the Toano Range, Nevada. Symbols as in Figure 4.

vitrophyres plus pyroclastic rocks are the result of differences in magma degassing. The pyroclastic rocks may be low simply because of degassing during eruption. The vitrophyres, which occur on the margin of the small plug and at the base of the lava flow related to the small plug, may represent an early volume of magma that lost more gas than later magma that filled the vent and capped the flows.

Because of its low boiling point, Hg is clearly a volatile element. The other anomalous elements are not generally considered to be volatile, but recent studies have demonstrated that many elements are transported in vapor phases associated with different types of cooling lava (cf. Stoiber and Rose, 1970, 1974; Keith et al., 1981; Oskarsson, 1981; Greenland and Aruscavage, 1986; Lowenstern et al., 1991). Symonds et al. (1987), who examined condensates, sublimates, and incrustations from fumaroles at Merapi, an andesitic stratovolcano in Indonesia, demonstrated that significant amounts of Au, As, and, to a lesser extent, Sb and many other elements can be transported in a magmatically derived vapor phase. Given that magma degassing can vary with time and that hydration of vitrophyres, vapor-phase crystallization, and devitrification can alter the chemical compositions of rocks, the magmatic abundances of those trace elements that are capable of being transported in significant quantities in a vapor phase, such as Hg, Au, As, and Sb, are uncertain. Additional work, including analyses of these elements in melt inclusions trapped in phenocrysts, as reported by Lowenstern et al. (1991) for Cu, is needed to determine true magmatic compositions.

RELATIONSHIP TO OTHER RHYOLITES

Rhyolites of the Toano Range are part of the latest series of magmatic events in northeastern Nevada (Stewart, 1980), but their relationship to other topaz rhyolites of the western United States is uncertain. Cenozoic magmatism in northeastern Nevada consisted of extrusion of late Eocene to Miocene andesites to rhyolites associated with subduction or early extension or both (Stewart, 1980; Miller, 1984; Seedorff, 1991) and a bimodal basalt-rhyolite suite associated with Basin and Range extensional tectonics. Additionally, the Snake River Plain 150 km to the north produced voluminous rhyolite and basalt associated with the eastward migration of the Yellowstone hot spot.

Coats (1987) mapped rhyolites of the Toano Range as part of his unit Tr_3, the youngest rhyolitic rocks of the region. The Toano rocks are, however, unlike rocks at other outcrops of Tr_3 that we have examined in the region, which consist of many types: more-or-less normal rhyolite lava flows, areally extensive rhyolite flows that resemble ash-flow tuffs in outcrop pattern, and rheomorphic ash-flow tuffs. Miller (1984) reported an age of 12.9 ± 0.4 Ma (K-Ar date on mixture of plagioclase and sanidine) for rhyolite of the Toano Range. This age is similar to those of many rhyolite lavas in nearby ranges. This regional outpouring of rhyolite is consistent with a genetic relationship to hot spot passage associated with development of the Snake River Plain. Topaz rhyolites associated with bimodal volcanism of the Snake River Plain include the Jarbidge Rhyolite in northeastern Nevada, which only locally contains topaz (Coats, 1964; Leeman, 1982; Christiansen et al., 1986), and possibly the Quaternary China Cap dome in the Blackfoot lava field in southeastern Idaho (Armstrong et al., 1975; Dayvault et al., 1984; Christiansen et al., 1986). Alternatively, the rhyolites of the Toano Range may be a newly recognized part of the large province of extension-related topaz rhyolites scattered throughout western Nevada and eastern Utah (Christiansen et al., 1986).

REFERENCES CITED

Armstrong, R.L., Leeman, W.P., and Malde, H.E. (1975) K-Ar dating, Quaternary and Neogene volcanic rocks of the Snake River Plain, Idaho. American Journal of Science, 275, 225–251.

Bonham, H.F., Jr., Garside, L.J., Hsu, L.C., Desilets, M., Price, J.G., Lechler, P.J., and Davis, D. (1990) Geochemical sampling and characterization of the Preble Formation. Nevada Bureau of Mines and Geology Open-File Report, 1-C93.

Christiansen, E.H., Bikun, J.V., Sheridan, M.F., and Burt, D.M. (1984) Geochemical evolution of topaz rhyolites from the Thomas Range and Spor Mountain, Utah. American Mineralogist, 69, 223–236.

Christiansen, E.H., Sheridan, M.F., and Burt, D.M. (1986) The geology and geochemistry of Cenozoic topaz rhyolites from the western United States. Geological Society of America Special Paper 205, 82 p.

Coats, R.R. (1964) Geology of the Jarbidge quadrangle, Nevada-Idaho. U.S. Geological Survey Bulletin 1141-M, 24 p.

———(1987) Geology of Elko County, Nevada. Nevada Bureau of Mines and Geology Bulletin 101, 112 p.

Dayvault, R.D., Rush, S.M., and Ludlam, J.R. (1984) Evaluation of uranium potential in a topaz-bearing rhyolite, China Hat dome, southeastern Idaho. Reports on field investigations of uranium anomalies, Bendix Field Engineering Corporation Open-File Report GJBX-1(84), II-1, II-26.

Duval, J.S. (1988) Aerial gamma-ray contour maps of regional surface concentrations of potassium, uranium, and thorium in Nevada. U.S. Geological Survey Geophysical Investigations Map GP-982, 1:750000 scale.

Glick, L.L. (1987) Structural geology of the northern Toano Range, Elko County, Nevada, 141 p. M.S. thesis, San Jose State University, San Jose, California.

Greenland, L.P., and Aruscavage, P. (1986) Volcanic emissions of Se, Te and As from Kilauea Volcano, Hawaii. Journal of Volcanology and Geothermal Research, 27, 195–201.

Keith, T.E.C., Casadevall, T.J., and Johnston, D.A. (1981) Fumarole encrustations: Occurrence, mineralogy, and chemistry. U.S. Geological Survey Professional Paper 1250, 239–250.

Lee, D.E., Kistler, R.W., Friedman, I., and Van Loenen, R.E. (1981) Two-mica granites of northeastern Nevada. Journal of Geophysical Research, 86, 10607–10616.

Leeman, W.P. (1982) Rhyolites of the Snake River Plain–Yellowstone Plateau province, Idaho and Wyoming. A summary of petrogenetic models. Idaho Bureau of Mines and Geology Bulletin 26, 203–212.

Lowenstern, J.B., Mahood, G.A., Rivers, M.L., and Sutton, S.R. (1991) Evidence for extreme partitioning of copper into a magmatic vapor phase. Science, 252, 1405–1409.

Miller, D.M. (1984) Sedimentary and igneous rocks of the Pilot Range and vicinity, Utah and Nevada. Utah Geological Association Publication 13, 45–63.

Miller, D.M., Nakata, J.K., and Glick, L.L. (1990) K-Ar ages of Jurassic to Tertiary plutonic and metamorphic rocks, northwestern Utah and northeastern Nevada. U.S. Geological Survey Bulletin 1906, 18 p.

Oskarsson, N. (1981) The chemistry of Icelandic lava incrustations and the latest stages of degassing. Journal of Volcanology and Geothermal Research, 10, 93–111.

Proffitt, J.L., Mayerson, D.L., Parker, D.P., Wolverson, N., Antrim, D., Berg, J., and Witzel, F. (1982) National uranium resource evaluation, Wells Quadrangle, Nevada, Idaho and Utah. Bendix Field Engineering Corporation Report PGJ/F-070(82), 36 p.

Seedorff, E. (1991) Magmatism, extension, and ore deposits of Eocene to Holocene age in the Great Basin—mutual effects and preliminary proposed genetic relationships. In G.L. Raines, R.E. Lisle, R.W. Schafer, and W.H. Wilkinson, Eds., Geology and ore deposits of the Great Basin: Symposium proceedings, p. 133–178. Geological Society of Nevada, Reno.

Stewart, J.H. (1980) Geology of Nevada, a discussion to accompany the geologic map of Nevada. Nevada Bureau of Mines and Geology Special Publication 4, 136 p.

Stoiber, R.E., and Rose, W.I., Jr. (1970) The geochemistry of Central American volcanic gas condensates. Geological Society of America Bulletin, 81, 2891–2911.

———(1974) Fumarole incrustations at active Central American volcanoes. Geochimica et Cosmochimica Acta, 38, 495–516.

Symonds, R.B., Rose, W.I., Reed, M.H., Lichte, F.E., and Finnegan, D.L. (1987) Volatilization, transport and sublimation of metallic and nonmetallic elements in high temperature gases at Merapi Volcano, Indonesia. Geochimica et Cosmochimica Acta, 51, 2083–2101.